Influence of Plastic Deformation of Particulates on Flexure Toughness of Brittle Matrix Composite

Yu Qiao[1]; Srinivas S. Chakravarthula[2]; and Xinguo Kong[3]

Abstract: In ductile-particulate reinforced composites with relatively low filler contents, the fracture toughness is dominated by the crack trapping effect. In this paper, this phenomenon is discussed in detail in context of R-curve analysis. The total fracture work is decomposed into the work of separation of matrix and the traction work associated with particulate rupture. It is concluded that, since the energy dissipation subsequent to the onset of unstable crack propagation does not affect the critical condition, the load bearing capacity of the particulates cannot be fully utilized. A closed-form expression relating the fracture toughness to the hardening behavior is obtained.

DOI: 10.1061/(ASCE)0733-9399(2005)131:3(319)

CE Database subject headings: Composite materials; Failure modes; Fracture mechanics; Stability analysis; Toughness; Deformation.

Introduction

Toughening brittle materials, such as cements and concretes, epoxy resin, and engineering ceramics by ductile particulates, has been an active research area for decades. The major attractions of particulate reinforced composites include the simplicity in processing and the excellent cost-performance balance. Depending on the properties of matrix and the processing conditions, the ductile particulates can be made from polymeric materials (Perek and Pilliar 1992; Cardwell and Yee 1998) or ductile metals and alloys (Jin and Batra 1999; Sabaizero and Pezzotti 2000; Bartolome et al. 2002; Gilbert et al. 2002). In these composites, the filler-matrix debonding is usually difficult and the fracture process is dominated by the plastic deformation of the particulates, especially when the particulates are reactive with the matrix and/or the strong interface bonds can be formed.

The toughening mechanism of the ductile particulates consists of the crack trapping effect and the bridging effect (Ravichandran 1992; Bao and Zok 1993). When a cleavage front encounters a particulate array, with increasing crack growth driving force, the front will bow into the brittle matrix between the particulates, as depicted in Fig. 1 (Mower and Argon 1995). At the verge of propagating, the local stress intensity factor equals the local fracture toughness, while at the concave sections the stress intensity factor is larger (Xu et al. 1998; Bower and Ortiz 1991). Thus, even without considering the additional work associated with particulate deformation and breakage, the average fracture resistance is higher than that of the matrix. With intermediate particulate volume fraction, the trapping effect can lead to a three-fold rise of fracture toughness over the neat matrix (Kotoul and Vrbka 2003; Qiao and Kong 2004). This type of front behavior is quite similar to that of a dislocation line sliding across a field of tough precipitates (Lange 1970), and similarly when the two front sections at both sides of a particulate merge together the crack front would bypass the particulate, leaving it behind the crack tip as a bridging reinforcement (Bower and Ortiz 1991; Mower and Argon 1995). A certain amount of fracture work is required to overcome the bridging force, leading to the further enhancement of fracture resistance. Usually, the bridging effect is pronounced when the filler content is high and, at the steady-state, the resistance can be larger than that of neat matrix by an order of magnitude (Qiao and Argon 2003; Qiao 2003a).

In engineering practice, however, if the filler content is high, the full development of filler-matrix bonding is difficult, and as a result the overall toughness can actually decrease as the particulate volume fraction increases (Cardwell and Yee 1998). In order to optimize the material performance, quite often the particulate volume fraction ranges from 0.1–5% (e.g., Bartolome et al. 2002; Gilbert et al. 2002). Under this condition, the particulates fail before the crack front can fully bypass them, and thus the trapping effect is dominant. Currently, in the discussion of front behavior, the particulates are usually assumed rigid, in which the influences of the strain hardening and the extensibility of particulates cannot be accounted for (e.g., Wu et al. 2002). While such models have been of unquestionable utility and are widely adhered to in discussing hard-particulate reinforced composites, they shed little light on the reliability analysis for composite materials toughened by deformable reinforcements.

In view of the above considerations, in the following sections, we will analyze the R-curve behavior of an array of ductile particulates in a brittle matrix composite under center-point bending, based on which the stability of crack advance and its dependence on hardening behavior of particulates will be studied in considerable detail. Fig. 2 shows a typical R-curve analysis. As the crack advances, due to a variety of mechanisms, such as process zone development and/or filler-matrix interaction, the fracture resis-

[1]Assistant Professor, Dept. of Civil Engineering, Univ. of Akron, Akron, OH 44325-3905. E-mail: yqiao@uakron.edu

[2]Graduate Student, Dept. of Civil Engineering, Univ. of Akron, Akron, OH 44325-3905.

[3]Graduate Student, Dept. of Civil Engineering, Univ. of Akron, Akron, OH 44325-3905.

Note. Associate Editor: Majid T. Manzari. Discussion open until August 1, 2005. Separate discussions must be submitted for individual papers. To extend the closing date by one month, a written request must be filed with the ASCE Managing Editor. The manuscript for this paper was submitted for review and possible publication on February 2, 2004; approved on August 6, 2004. This paper is part of the ***Journal of Engineering Mechanics***, Vol. 131, No. 3, March 1, 2005. ©ASCE, ISSN 0733-9399/2005/3-319–323/$25.00.

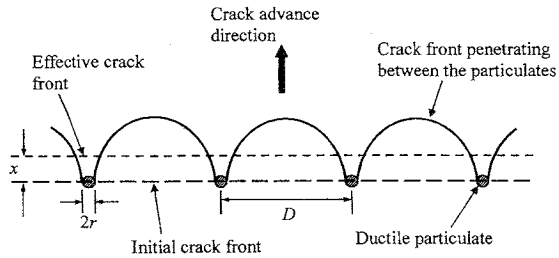

Fig. 1. Schematic diagram of the crack front penetrating between the particulates

tance of the material, R, can increase with the crack growth distance (McClintock and Argon 1993). Note that the energy release rate, G, is also a function of the crack length, a. When the external load $P=P_1$ is low, $G<R$ at $a=a_0$, with a_0 being the initial crack length, and the crack will not propagate. As P rises, $G(a_0)$ keeps increasing. When $P=P_i$, G reaches $R(a_0)$ and the crack grows. Since the fracture resistance increases more rapidly than the energy release rate, the crack will immediately stop until the external load further increases such that

$$G=R \tag{1}$$

is satisfied, i.e., the crack growth is stable. With increasing a, the increasing rate of energy release rate rises and that of fracture resistance decreases. Eventually, when $P=P_{cr}$,

$$\frac{\partial G}{\partial a}=\frac{\partial R}{\partial a}, \tag{2}$$

and the crack advance becomes unstable (Hellan 1984).

Peak Resistance of a Regular Array of Ductile Particulates

For structural materials, the reliability is often measured by the flexure toughness. Consider the center-point bending arrangement where the precrack along the median plane is subjected to tensile stresses [see Fig. 3(a)]. In order to study the barrier effect, we assume that initially the crack tip is arrested by a regular array of ductile particulates. The matrix is brittle and the fracture mode in matrix is cleavage. The particulate size is much smaller than the process zone size such that the average crack tip stress field can be defined.

As the center-point load, P, rises, the stress intensity at the crack front keeps increasing. When the local stress intensity factor

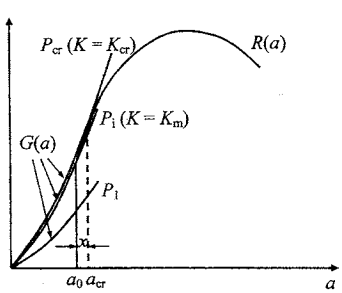

Fig. 2. Typical R-curve analysis. The crack starts to grow stably when the effective stress intensity factor $K=K_m$, and the crack advance becomes unstable as $K=K_{cr}$.

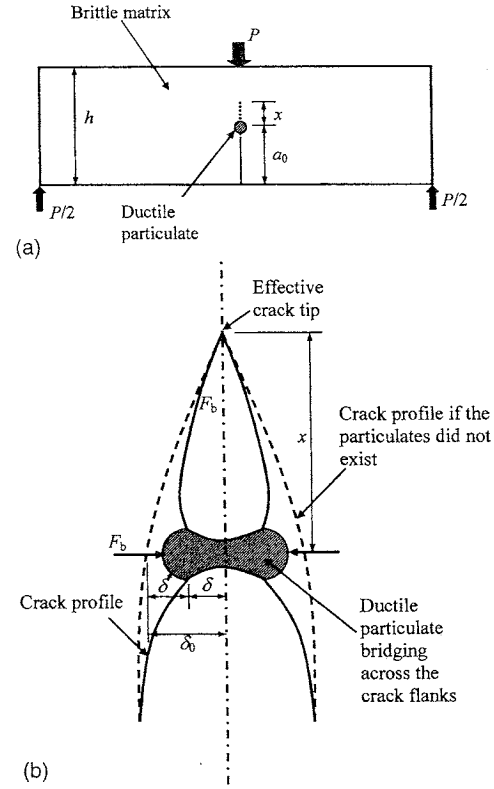

Fig. 3. Schematic diagrams of (a) the crack overcoming an array of ductile particulates in a flexure toughness measurement setup; and (b) the deformation of the ductile particulates behind the effective crack tip

reaches the fracture toughness of the matrix, K_m, the crack front starts to penetrate stably between the particulates with the parts trapped by the particulates pinned behind the verge of propagating, leading to the effective crack advance distance, x, as observed by Mower and Argon (1995) and simulated by Bower and Ortiz (1991). The effective crack front can be somewhat arbitrarily defined as the line passing through the centroids of the cleavage facets ahead of the particulate array.

With the stable crack growth, the particulates are left behind the effective crack tip and subjected to the bridging force, F_b. When $F_b \leq \sigma_0(\pi r^2)$, with r being the particulate radius and σ_0 the yield strength, the particulates deform elastically. As F_b exceeds this critical value, plastic deformation will occur, as shown in Fig. 3(b). The strain hardening behavior of the particulates can be assumed to be

$$\frac{\sigma}{\sigma_0}=\left(\frac{\varepsilon}{\varepsilon_0}\right)^n \tag{3}$$

where σ and ε=bridging stress and strain, respectively; $\varepsilon_0=\sigma_0/E_p$=yield strain; E_p=Young's modulus of particulate; and n=material constant. Once the ultimate strength of particulates is reached, the strain softening will result in a decrease in fracture resistance. Note that, since, as shown in Fig. 2, the descending part of $R(a)$ has little effect on the critical condition of Eqs. (1) and (2), only the strain hardening stage of the σ-ε curve is relevant to the calculation of the fracture resistance.

The fracture work associated with the crack growth distance, x, can be stated as (Qiao 2003b)

$$W = G_m x + \frac{1}{D}\int_0^{\delta} F_b d\delta \tag{4}$$

where W=fracture work per unit thickness; G_m=work of separation of the matrix; D=the average particulate spacing; and δ=crack opening displacement. Note that the effective crack length $a=a_0+x$. The fracture resistance, R, can then be obtained as

$$R = \frac{\partial W}{\partial a} = G_m + \frac{F_b}{D}\frac{\partial \delta}{\partial a} \tag{5}$$

According to Eq. (3), the bridging force is related to δ

$$F_b = \sigma_0(\pi r^2)\left(\frac{\delta - \delta_1}{\delta_1 \varepsilon_0}\right)^n, \tag{6}$$

where δ_1=initial crack opening displacement. Thus, the resistance curve can be rewritten as

$$R = G_m + \frac{\sigma_0(\pi r^2)}{D}\left(\frac{\delta - \delta_1}{\delta_1 \varepsilon_0}\right)^n \frac{\partial \delta}{\partial a} \tag{7}$$

and, therefore,

$$\frac{\partial R}{\partial a} = \frac{\sigma_0 n(\pi r^2)}{D\delta_1 \varepsilon_0}\left(\frac{\delta - \delta_1}{\delta_1 \varepsilon_0}\right)^{n-1}\frac{\partial \delta}{\partial a} + \frac{\sigma_0(\pi r^2)}{D}\left(\frac{\delta - \delta_1}{\delta_1 \varepsilon_0}\right)^n \frac{\partial^2 \delta}{\partial a^2} \tag{8}$$

The effective stress intensity factor caused by the bridging force is (Hellan 1984)

$$K_b = \frac{F_b}{D\sqrt{\pi a}}\sqrt{1 + 2\frac{a_0}{x}}, \tag{9}$$

and, consequently, the associated elastic energy per unit thickness can be obtained as

$$U_b = \frac{1-\nu^2}{E}\frac{F_b^2}{\pi D^2}\ln\frac{1+\tilde{x}}{\tilde{x}^2} \tag{10}$$

where $\tilde{x}=x/a_0$; and E and ν=modulus of elasticity and Poisson's ratio of the matrix, respectively. Since the matrix is linear elastic, $U_b=F_b\delta^*/D$, where δ^*=change in crack opening displacement caused by F_b [see Fig. 3(b)], which, combined with Eq. (10), leads to

$$\delta^* = \frac{1-\nu^2}{\pi E D}F_b \ln\frac{1+\tilde{x}}{\tilde{x}^2} \tag{11}$$

If the bridging particulates did not exist, the crack opening displacement at a point x apart from the crack tip can be calculated as (Ulfyand 1965)

$$\delta_0(x) = \frac{1-\nu}{\mu}\left(2K\sqrt{\frac{x}{2\pi}}\right) \tag{12}$$

where μ=shear modulus of the matrix and

$$K = 3.75\frac{Ph}{(h-a)^{3/2}} \tag{13}$$

is the effective stress intensity factor (Gross and Srawley 1972), where P=the center-point load per unit thickness; h=beam height; a=effective crack length in the range of $0.4h$ to $0.6h$; and the beam length=$4h$. Note that $\delta_0=\delta+\delta^*$. Hence, through Eqs. (6), (11), and (12), we have

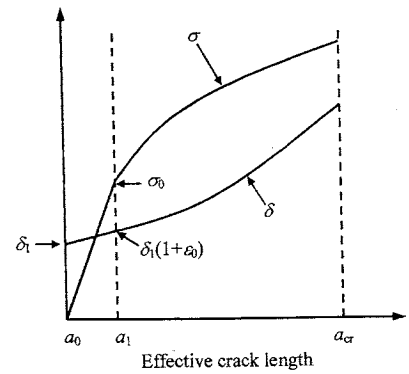

Fig. 4. Evolution of the bridging force and the crack opening displacement as the crack advances

$$\varepsilon_0\delta_1\left(\frac{F_b}{\pi r^2\sigma_0}\right)^{1/n} + \frac{1-\nu^2}{\pi D E}F_b \ln\frac{1+\tilde{x}}{\tilde{x}^2} = \frac{1-\nu}{\mu}\frac{7.5Ph}{(h-a)^{3/2}}\sqrt{\frac{x}{2\pi}} - \delta_1 \tag{14}$$

through which F_b and δ can be obtained as functions of a. Fig. 4 depicts the evolution of δ and σ in the framework defined above. Initially, at the onset of stable crack growth, the traction is zero and the crack opening displacement is δ_1, which can be estimated as $\delta_1=(K_m/\sigma_m)^2/2\pi$, with K_m and σ_m being the fracture toughness and the yield strength of the matrix, respectively. As the crack advances, σ and δ keep increasing. When $a=a_1$, $\sigma=\sigma_0$ and the particulates yield. The associated crack opening displacement is $\delta=\delta_1(1+\varepsilon_0)$. Eventually, when $a=a_{cr}$, the criterion of unstable crack propagation is satisfied and the material fails. It will be shown shortly that at a_{cr}, the bridging stress is lower than the ultimate strength σ_u, indicating that the load bearing capacity of the particulates is not fully utilized. Since, as will be shown shortly, a_1-a_0 is much smaller than $a_{cr}-a_0$, the linear stage will be neglected in the following discussion.

The overall strain energy consists of two parts: The strain energy caused by the external load, U_{np}, and the portion caused by the bridging force in the particulates, U_b. Through Eq. (13), the energy release rate associated with P can be obtained as $G_{np}=(1-\nu^2/E)(14P^2h^2/(h-a)^3)$, and since $G_{np}=-\partial U_{np}/\partial a$, we have

$$U_{np} = U^* - \frac{1-\nu^2}{E}\frac{7P^2h^2}{(h-a)^2} \tag{15}$$

where U^*=parameter independent of a. The combination of Eqs. (10) and (15) gives the crack growth driving force

$$G = -\frac{\partial(U_{np}+U_b)}{\partial a} = \frac{1-\nu^2}{E}\frac{14P^2h^2}{(h-a)^3} - \frac{1-\nu^2}{\pi D^2 E}\left[2F_b\frac{\partial F_b}{\partial a}\ln\frac{1+\tilde{x}}{\tilde{x}^2} - \frac{F_b^2}{1+\tilde{x}}\frac{\tilde{x}+2}{a_0\tilde{x}}\right] \tag{16}$$

The changing rate of G can then be obtained as

$$\frac{\partial G}{\partial a} = \frac{1-\nu^2}{E}\frac{42P^2h^2}{(h-a)^4} - \frac{1-\nu^2}{\pi D^2 E}\left\{2\left[\left(\frac{\partial F_b}{\partial a}\right)^2 + F_b\frac{\partial^2 F_b}{\partial a^2}\right]\ln\frac{1+\tilde{x}}{\tilde{x}^2} - \frac{2F_b}{a_0}\frac{\partial F_b}{\partial a}\frac{\tilde{x}+2}{\tilde{x}(\tilde{x}+1)} + \frac{F_b^2}{a_0^2}\frac{\tilde{x}^2+4\tilde{x}+2}{\tilde{x}^2(\tilde{x}+1)^2}\right\} \tag{17}$$

Substitution of Eqs. (7) and (16) into Eq. (1) and Eqs. (8) and (17) into Eq. (2), with F_b and δ given by Eqs. (6) and (14), gives the critical center-point load, P_{cr}, and the critical crack length, a_{cr},

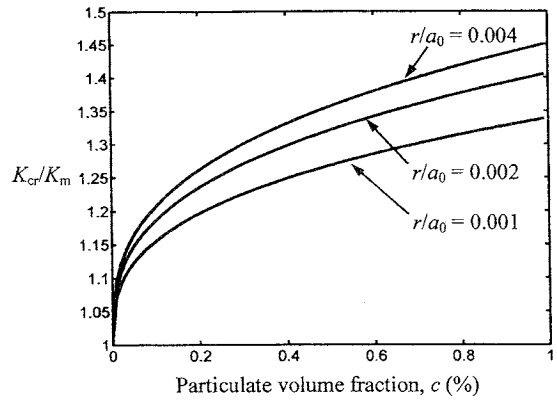

Fig. 5. Fracture toughness as function of particulate volume fraction and size

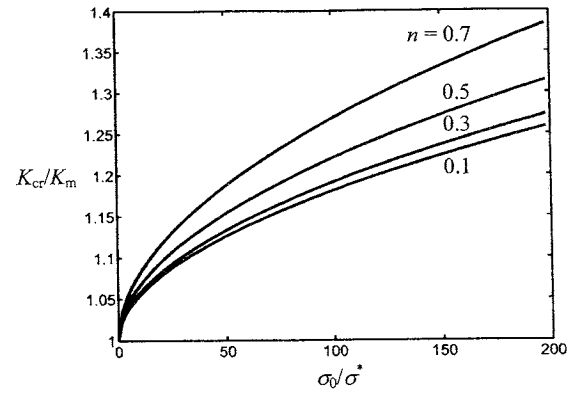

Fig. 6. Effects of strength and strain hardening of the particulates on the fracture toughness

associated with the unstable crack advance, based on which the critical stress intensity factor, K_{cr}, offered by the array of ductile particulates can be calculated through Eq. (13).

Results and Discussion

Fig. 5 shows the numerical result of the fracture toughness as a function of particulate volume fraction, c, and particulate radius, r. Note that for spherical particulates, c can be related to r and D through $c=4\pi r^3/(3D^3)$. The value of n is set to 0.3. As c increases, the spacing among the particulates tends to decrease and the fracture toughness rises, which is consistent with the assumption that the particulate-matrix bonding is perfect. The result of a_{cr} shows that $a_{cr}-a_0$ is indeed much larger than a_1-a_0, indicating that the above discussion is self-compatible. Note that when the particulate volume fraction is relatively large, full wetting at the filler-matrix interface can be difficult and the fracture toughness can decrease with increasing c. Under this condition, the failure behavior is dominated by debonding and this model is no longer valid.

According to Eq. (6), the toughening effect of a larger particulate is more pronounced than that of a smaller one. However, with a constant particulate volume fraction, as the particulates become larger the number density is lowered, which tends to reduce the fracture toughness. Through Fig. 5, it can be seen that K_{cr} increases with r, that is, the former effect is dominant. This phenomenon should be attributed to the nonlinear characteristic of the crack-particulate interaction captured in Eq. (4). The effective traction work is determined by F_b/D, where F_b is proportional to r^2 while D is proportional to $c^{1/3}$, giving the increase in r more weight than the decrease in D. Notice that when c is small $\partial K_{cr}/\partial c$ is quite large and the level of uncertainty in the measurement of c can be high.

The effects of the properties of particulates, which are characterized by σ_0 and n, are shown in Fig. 6, where the characteristic stress $\sigma^*=1$ MPa. The particulate volume fraction is taken as 0.5%. The result demonstrates clearly that the degree of toughening increases with both σ_0 and n, as it should. When the particulate strength is low, K_{cr} rises rapidly as σ_0 increases, and reaches a quasi-steady state when σ_0 exceeds a critical value. On the other hand, K_{cr} is somewhat insensitive to the change in n when $n<0.3$.

As depicted in Fig. 4, with increasing crack extension the elongation of the particulates increases monotonically. In the optimum case where the load bearing capacity of the particulates is fully utilized, the unstable crack advance occurs simultaneously as the particulates break up through rupture. However, according to Fig. 2 the critical condition of $\partial G/\partial a=\partial R/\partial a$ must be satisfied prior to the onset of strain softening, after which the work of separation can be compensated spontaneously by the release of the strain energy stored in the specimen and contributes little to K_{cr}. Actually, in the calculations discussed above, it was found that when both Eqs. (1) and (2) are satisfied the strain of particulate is always much lower than the strain of softening, indicating that the toughening effect is independent of the extensibility of the particulates.

It has been well known that R-curve analysis will result in a size dependence of fracture toughness. The factors of a_0 and h come in by affecting the changing rate of energy release rate, $\partial G/\partial a$. As shown in Fig. 2 and Eq. (17), both G and $\partial G/\partial a$ change with a_0 and h, while R and $\partial R/\partial a$ are independent of the sample geometry. Thus, with everything else the same, the critical condition of Eqs. (1) and (2) can be satisfied at lower values of P_{cr} and a_{cr} with a higher a_0/h ratio, which leads to a smaller K_{cr} (see Fig. 7). This size effect can also be attributed to the nonself-similar nature of the crack advance, since the size and spacing of particulates remain the same as the crack length varies. However, through Fig. 7, it can be seen that in the range of a_0/h under consideration, the crack length dependence of fracture toughness is negligible.

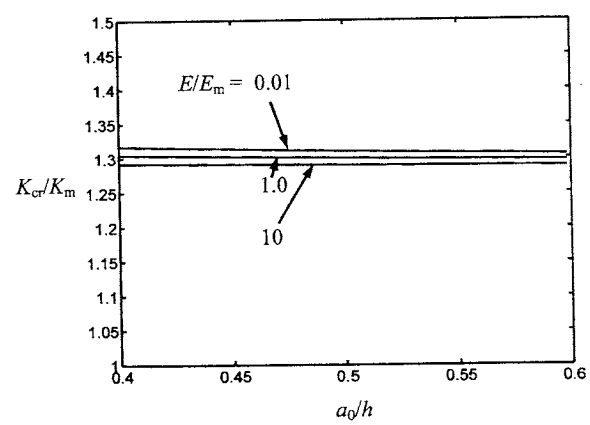

Fig. 7. Influences of the initial crack length and the matrix stiffness on the fracture toughness

Fig. 7 also indicates that K_{cr} decreases with increasing modulus of elasticity of the matrix. As the matrix becomes increasingly compliant, the particulates look "stiffer" and thus the toughening effect is more significant. However, the E dependence of K_{cr} is quite weak. As E increases by a factor of 1,000, the change in K_{cr}/K_m is only about 5%. The numerical result also shows that K_{cr} is nearly independent of the Poisson's ratio of the matrix.

Since the fracture toughness is insensitive to E, ν, a_0, and h, the vital factors that govern K_{cr} are $\{\sigma_0, n, r, c, K_m\}$, among which σ_0 and n capture the particulate properties, r and c reflect the microstructure, and K_m describes the matrix behavior. Through the Π theorem (Thomas 1997), we have $K_{cr}/K_m = f(n, \sigma_0\sqrt{r}/K_m, c)$, where f is a function to be determined. By using a two-power-law function, we may state that

$$\frac{K_{cr}}{K_m} = \alpha(n) \cdot \left(\frac{\sigma_0\sqrt{r}}{K_m}\right)^{\beta_1} c^{\beta_2} \tag{18}$$

where α=function of n; and β_1 and β_2=two material constants. By comparing with the numerical results using the least-squares method, these parameters can be determined as $\alpha(n)=0.81-0.22n+1.1n^2$, and β_1 and β_2 are in the range of 0.25–0.75.

Clearly, the above discussion based on the line average approximation cannot be extended to the high filler content composites and, even when the filler content is low, this model does not provide an "exact" solution for the fracture toughness. Nevertheless, it gives the closed-form expression relating K_{cr} to the mechanical properties of the particulates, based on which a quick assessment of the effectiveness of the design variables can be performed.

Conclusions

In this paper, the flexure toughness of brittle matrix composites reinforced by deformable particulates is discussed in context of R-curve analysis. The effective resistance offered by a regular array of particulates to cleavage cracking is taken as the critical energy release rate at the onset of unstable crack advance, through which the influences of the strength, hardening behavior, size, and volume fraction of the particulates, as well as the matrix properties can be evaluated. The work of separation associated with the unstable crack propagation is related to the strain energy stored in the sample prior to the critical condition and, therefore, the fracture toughness mostly depends on the early stage of the plastic deformation of the particulates. The following conclusions are drawn:

(1) The trapping effect of the ductile particulates in brittle matrix can be described by a two-power-law function quite well.
(2) To enhance the fracture toughness, the particulates should be of high yield strength and pronounced strain hardening characteristic.
(3) Since the fracture work subsequent to the onset of unstable crack advance is not related to the external loading, K_{cr} is somewhat independent of the extensibility of the particulates.
(4) The fracture toughness increases with the particulate volume fraction with a descending rate.
(5) With the same particulate volume fraction, increasing particulate size has a beneficial effect to the fracture resistance.
(6) The fracture toughness is insensitive to the elastic properties of the matrix.

Acknowledgment

This work was recently supported by the National Science Foundation under Grant No. CMS-0408276.

References

Bao, G., and Zok, F. (1993). "On the strength of ductile particulate-reinforced brittle-matrix composites." *Acta Metall. Mater.*, 41(12), 3515–3524.

Bartolome, J. F., Diaz, M., and Moya, J. S. (2002). "Influence of the metal particulate size on the crack growth resistance in mullite-molybdenum composites." *J. Am. Ceram. Soc.*, 85(11), 2778–2784.

Bower, A. F., and Ortiz, M. (1991). "A three-dimensional analysis of crack trapping and bridging by tough particles." *J. Mech. Phys. Solids*, 39(6), 815–858.

Cardwell, B. J., and Yee, A. F. (1998). "Toughening of epoxies through thermoplastic crack bridging." *J. Mater. Sci.*, 33(22), 5473–5484.

Gilbert, E. N., Hayes, B. S., and Seferis, J. C. (2002). "Variable density composite systems constructed by metal particulate modified prepregs." *J. Compos. Mater.*, 36(17), 2045–2060.

Gross, B., and Srawley, J. E. (1972). "Stress intensity factor for bend and compact specimens." *Eng. Fract. Mech.*, 4(3), 587–589.

Hellan, K. (1984). *Introduction to fracture mechanics*, McGraw–Hill, NY.

Jin, Z. H., and Batra, R. C. (1999). "Thermal shock cracking in a metal-particulate-reinforced ceramic matrix composite." *Eng. Fract. Mech.*, 62, 339–350.

Kotoul, M., and Vrbka, J. (2003). "Crack bridging and trapping mechanisms used to toughen brittle matrix composite." *Theor. Appl. Fract. Mech.*, 40(1), 23–44.

Lange, F. F. (1970). "The interaction of a crack front with a second phase dispersion." *Philos. Mag.*, 22, 983–992.

McClintock, F. A., and Argon, A. S. (1993). *Mechanical behavior of materials*, CBLS, Marietta, OH.

Mower, T. M., and Argon, A. S. (1995). "Experimental investigations of crack trapping in brittle heterogeneous solids." *Mech. Mater.*, 19, 343–364.

Perek, J., and Pilliar, R. M. (1992). "Fracture toughness of composite acrylic bone cements." *J. Mater. Sci.*, 3(5), 333–344.

Qiao, Y. (2003a). "Fracture toughness of composite materials reinforced by debondable particulates." *Scr. Mater.*, 49, 491–496.

Qiao, Y. (2003b). "Modeling of resistance curve of high-angle grain boundary in Fe-3 wt %Si alloy." *Mater. Sci. Eng., A*, 361, 350–357.

Qiao, Y., and Argon, A. S. (2003). "Cleavage cracking resistance of high angle grain boundaries in Fe-3 wt %Si alloy." *Mech. Mater.*, 35, 313–331.

Qiao, Y., and Kong, X. (2004). "Unstable crack advance across a regular array of short fibers in brittle matrix." *Compos. Sci. Technol.*, 64, 711–717.

Ravichandran, K. S. (1992). "The mechanics of toughness development in ductile phase reinforced brittle matrix composites." *Acta Metall. Mater.*, 40(5), 1009–1022.

Sabaizero, O., and Pezzotti, G. (2000). "Influence of the metal particulate size on toughness of Al_2O_3/Mo composite." *Acta Mater.*, 48(4), 985–992.

Thomas, S. (1997). *Applied modeling and dimensional analysis*, McGraw–Hill, NY.

Ulfyand, Y. S. (1965). *Survey of articles on the application of integral transforms in theory of elasticity*, Univ. of North Carolina, Raleigh, NC.

Wu, W., Sadeghipour, K., Boberick, K., and Baran, G. (2002). "Predictive modeling of elastic properties of particulate-reinforced composites." *Mater. Sci. Eng., A*, 332, 362–370.

Xu, G., Bower, A. F., and Ortiz, M. (1998). "The influence of crack trapping on the thoughness of fiber reinforced composites." *J. Mech. Phys. Solids*, 46(10), 1815–1833.